

## Supporting Information

### **Siloxane Engineered Polydiketopyrrolopyrrole Derivatives with Improved Crystallinity and Doping Efficiency for Thermoelectric Power Generation**

Shabab Hussain<sup>a,b,c,d,†</sup>, Yufeng Wu<sup>b,‡</sup>, Zhifu Chen<sup>b</sup>, Zhiyong Luo<sup>b</sup>, Fei Zhong<sup>c</sup>, Yu Chen<sup>a,\*</sup>,  
Chunmei Gao<sup>b,\*</sup> and Lei Wang<sup>c</sup>

<sup>a</sup> School of Chemistry and Environmental Engineering, Hanshan Normal University, Chaozhou, Guangdong 521041, P. R. China.

<sup>b</sup> College of Chemistry and Environmental Engineering, Shenzhen University, Shenzhen 518060, P. R. China.

<sup>c</sup> Shenzhen Key Laboratory of Polymer Science and Technology, College of Materials Science and Engineering, Shenzhen University, Shenzhen 518060, P. R. China.

<sup>d</sup> College of Physics and Optoelectronic Engineering, Shenzhen University, Shenzhen, 518060, P. R. China.

#### **Corresponding Author**

\*E-mail addresses: [2639@hstc.edu.cn](mailto:2639@hstc.edu.cn) (Y. Chen), [gaocm@szu.edu.cn](mailto:gaocm@szu.edu.cn) (C. Gao)

<sup>‡</sup>These two authors contributed equally.

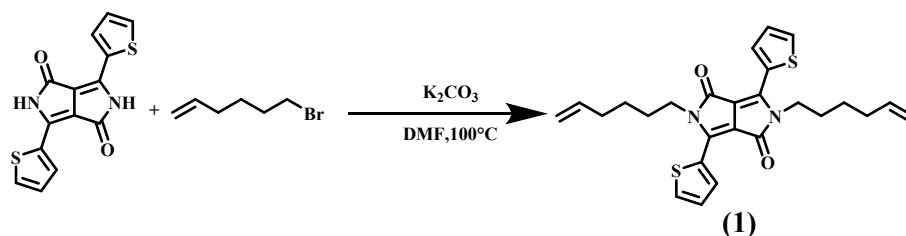
## S1. Experimental section

### S1.1. Materials

Ethanol, methanol, acetonitrile, di/tri-chloromethane, n-hexane, acetone, deuterated chloroform, deionized (DI) water, ligroin, chlorobenzene, and O-dichlorobenzene were bought from Aladdin Chemicals. All solvents were analytical grade. Potassium carbonate, magnesium sulfate, sodium sulfate, ferric chloride, tetrabutylhexafluorophosphateamine, N-butyltrichlorosilane, platinum(0)-1,3-diethylene-1,1,3,3-tetramethyldisiloxane complex (in Xylene, Pt ~2%), 6-Bromo-1-hexene, 3,6-Bis(2-thienyl)-2,5-dihydropyrrole[3,4-c]pyrrole-1,4-dione, 3,6-Bis(5-bromothiophene-2-yl)-2,5-bis(2-decyltetradecyl)pyrrolo[3,4-c]pyrrole-1,4-dione, 2,5-Bis(trimethyltyl)thiophene, Tris(o-methylphenyl) phosphorus, and Tris(dibenzylbenzylacetone) palladium were purchased from Jiangsu Jia Biotechnology Co., Ltd.

### S1.2. Synthesis and NMR characterization of DPP reactants/monomers

#### S1.2.1. Compound 1 (2,5-di(hex-5-en-1-yl)-3,6-di(thiophen-2-yl)-2,5-dihydropyrrolo[3,4-c]pyrrole-1,4-dione).



3,6-bis(2-thienyl)-2,5-dihydropyrrolo[3,4-c]pyrrole-1,4-dione (1.00 g, 3.33 mmol) and anhydrous potassium carbonate (1.84 g, 13.32 mmol) were taken in the 100 mL dry Schlenk tube. 6-bromo-1-hexene (1.81 mL, 13.32 mmol) was added through the pipette, and argon gas was fed into the

Schlenk tube for 10 min to remove the air. Subsequently, 20 mL anhydrous N, N-dimethylformamide (DMF) was added and the reaction was stirred magnetically at 100 °C overnight. TLC plates were employed to monitor the reaction. After the reaction is complete, the reaction mixture was cooled to room temperature and was poured into a separating funnel. The reaction mixture was extracted twice with dichloromethane (DCM) and deionized (DI) water, respectively. Finally, the reaction mixture was extracted again with saturated salt water, and the organic liquid phase was obtained by drying with anhydrous magnesium sulfate. After drying, the reaction mixture was filtered and concentrated, and the obtained crude product was further purified by column chromatography (CC). The eluent was petroleum ether (PE):DCM = 1:1 (volume ratio). The purified solution was concentrated by rotary evaporator. After drying, black purple solid was obtained with mass of 1.20 g and yield of 77.57%.

The hydrogen NMR spectrum of compound 1 is shown in **Fig. S1** with the following chemical shifts:  $^1\text{H}$  NMR (400 MHz,  $\text{CDCl}_3$ )  $\delta$  8.92 (d, 2H), 7.64 (d, 2H), 7.30-7.27 (d, 2H), 5.79 (m, 2H), 5.04-4.92 (m, 4H), 4.13-4.06 (m, 4H), 2.11 (m, 4H), 1.77 (m, 4H), 1.55-1.50 (m, 4H).

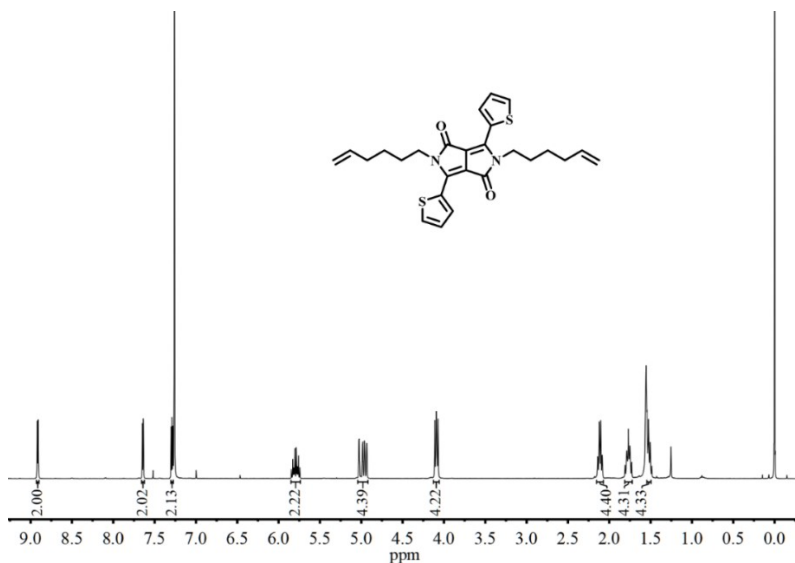
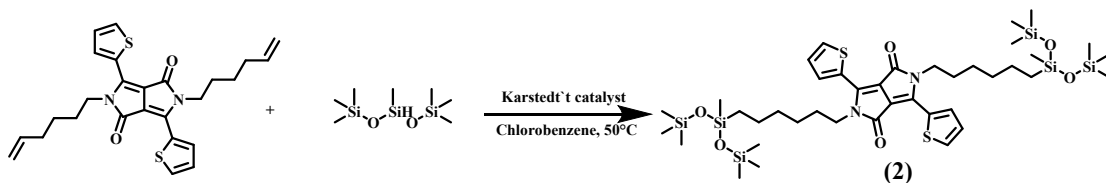


**Fig. S1.**  $^1\text{H}$  NMR of compound 1.

**S1.2.2. Compound 2 (2,5-bis(6-(1,1,3,5,5,5-heptamethyltrisiloxan-3-yl)hexyl)-3,6-di(thiophen-2-yl)-2,5-dihydropyrrolo[3,4-c]pyrrole-1,4-dione).**



Compound 1 (1.00 g, 2.15 mmol) was added into the 100 mL Schlenk tube with the addition of 20 mL anhydrous chlorobenzene. Prior to dissolution of compound 1, the water vapors and oxygen content (air) were removed. After the complete dissolution of compound 1, heptamethyltrisiloxane (1.75 mL, 6.46 mmol) was added into the reactor *via* syringe along with the addition of 10  $\mu\text{L}$  of Karstedt's catalyst. The mixture was stirred at 50  $^{\circ}\text{C}$  overnight. After the reaction is complete, the reaction mixture was cooled to room temperature, and was evaporated under reduced pressure to obtain crude product, which was further purified by CC, the eluent was PE:DCM = 2:1 (volume

ratio). Finally, the resulting purified liquid was concentrated and dried to obtain a black-purple solid with mass of 1.69 g and yield of 86.07%.

The hydrogen NMR spectrum of compound 2 is shown in **Fig. S2** with the following chemical shifts:  $^1\text{H}$  NMR (400 MHz,  $\text{CDCl}_3$ )  $\delta$  8.93 (d, 2H), 7.64 (d, 2H), 7.30-7.27 (m, 2H), 4.10-4.04 (m, 4H), 1.78-1.70 (m, 4H), 1.41-1.28 (m, 12H), 0.47-0.42 (m, 4H), 0.07 (s, 36H), -0.02 (s, 6H).

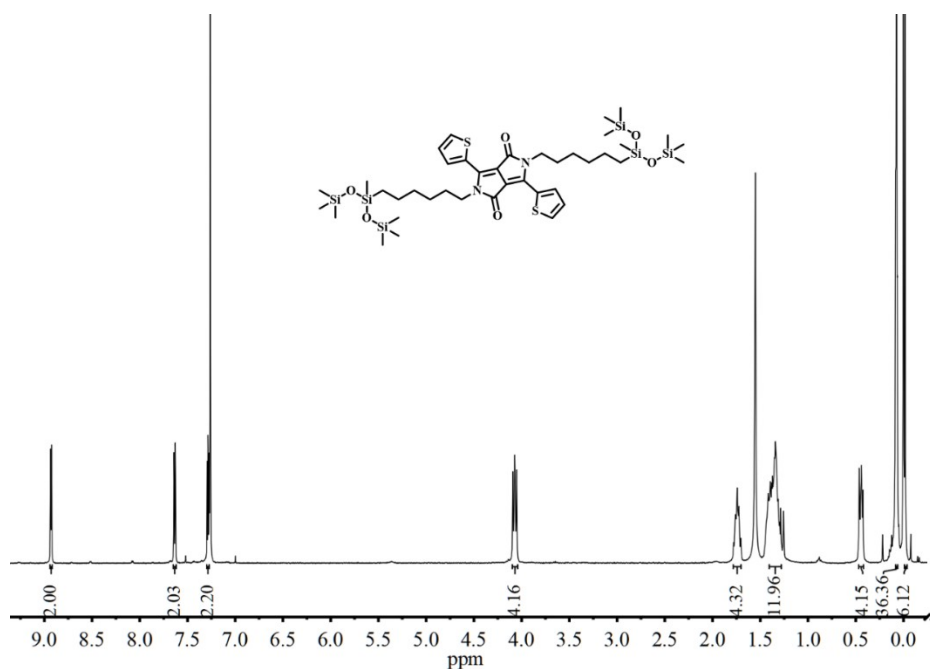
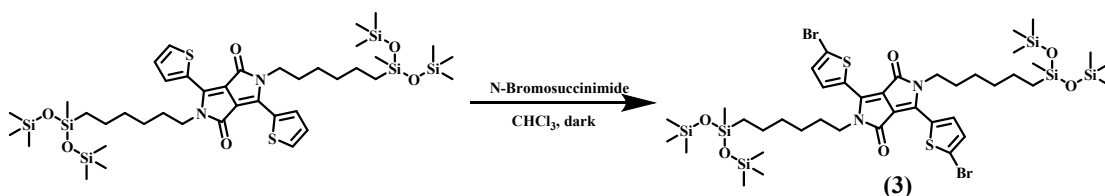


**Fig. S2.**  $^1\text{H}$  NMR of compound 2.

**S1.2.3. Compound 3 (3,6-bis(5-bromothiophen-2-yl)-2,5-bis(6-(1,1,1,3,5,5,5-heptamethyltrisiloxan-3-yl)hexyl)-2,5-dihydropyrrolo[3,4-c]pyrrole-1,4-dione).**



Compound 2 (0.80 g, 0.879 mmol) was added to a 100 mL Schlenk tube with the addition of N-bromosuccinimide (NBS) (391.32 mg, 2.20 mmol). The reactor was wrapped with Tin foil to protect from light. 15 mL of chloroform was slowly added into the reactor, and the reaction was stirred at 60 °C for 30 min. The cooled reaction mixture was poured into the separating funnel, and was extracted twice with DCM and DI water, respectively. In addition, the reaction solution was re-extracted with saturated salt water, and the organic phase was dried with anhydrous magnesium sulfate, filtered, and concentrated. The obtained crude product was further purified by CC with the eluent of PE:DCM = 1:3 (volume ratio). At last, the obtained organic liquid phase was concentrated and dried. 0.548 slightly viscous black-purple solid with yield of 58.43 % was obtained.

The hydrogen NMR spectrum of compound 3 is shown in **Fig. S3**, and the chemical shifts are as follows:  $^1\text{H}$  NMR (400 MHz,  $\text{CDCl}_3$ )  $\delta$  8.69 (d, 2H), 7.25 (d, 2H), 4.03-3.96 (m, 4H), 1.72 (m, 4H), 1.39-1.28 (m, 12H), 0.49-0.43 (m, 4H), 0.09 (s, 36H), -0.01 (s, 6H).

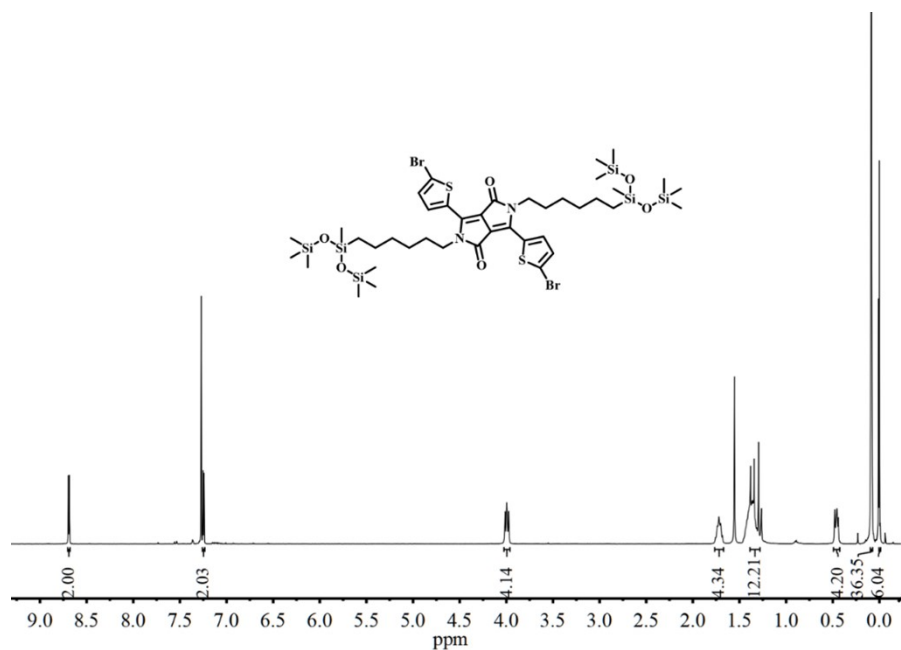


**Fig. S3.**  $^1\text{H}$  NMR of compound 3.

### S1.3. Synthesis and NMR characterization of polymers containing siloxane Side chains

In order to synthesize polymers of different proportions using the Stille coupling method, a clean Schlenk tube was filled with the following chemicals: (i) compound 3 (mass equivalent,  $m = 0.1, 0.3, 0.5, 0.7$ ) 3,6-bis(5-bromothiophene-2-yl)-2,5-bis(2-decyltetradecyl)pyrrolo[3,4-c]pyrrole-1,4-dione (1-m equivalent); (ii) 2,5-bis(trimethyltinyl)thiophene (1-m equivalent); (iii) catalysts tris(*o*-methylphenyl)phosphorus ( $P(\text{otol})_3$ , 0.08-m equivalent); and (iv) tris(dibenzylbenzylacetone)palladium ( $\text{Pd}_2(\text{dba})_3$ , 0.02-m equivalent), as shown in **Scheme 1** (See the manuscript). The Schlenk tubes were first vacuumed and then purged with nitrogen. This process was repeated three times to expel the oxygen and water vapors from the Schlenk tube. Afterwards, 4 mL anhydrous chlorobenzene was injected into the tubes with needles. The reaction was stirred at 120 °C for 6 h. After the reaction was cooled to room temperature, a certain amount of methanol was added to precipitate the final product. The reaction mixture was filtered to obtain the final crude polymer. The filtered polymer was finally extracted by Soxhlet extraction with methanol, acetone, and *n*-hexane. Therefore, the final products namely “PDPPSi<sub>0</sub>”, “PDPPSi<sub>10</sub>”, “PDPPSi<sub>30</sub>”, “PDPPSi<sub>50</sub>”, and “PDPPSi<sub>70</sub>” were vacuum dried. The <sup>1</sup>H-NMR characterization of polymers with different siloxane side chain content is as follows:

*PDPPSi<sub>0</sub>*

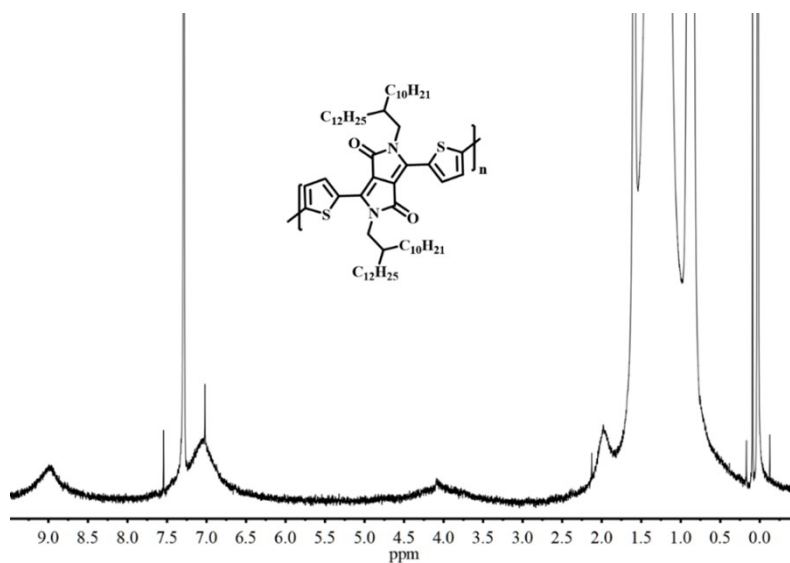


**Fig. S4.** <sup>1</sup>H NMR spectrum of polymer PDPPSi<sub>0</sub>.

The <sup>1</sup>H NMR spectra of PDPPSi<sub>0</sub> (black bulk solid, 61% yield) is shown in **Fig. S4**. <sup>1</sup>H NMR (400 MHz, CDCl<sub>3</sub>) δ 8.96 (s, 2H), 7.02 (s, 4H), 4.09 (s, 4H), 2.06-0.40 (m, alkyl).

*PDPPSi<sub>10</sub>*

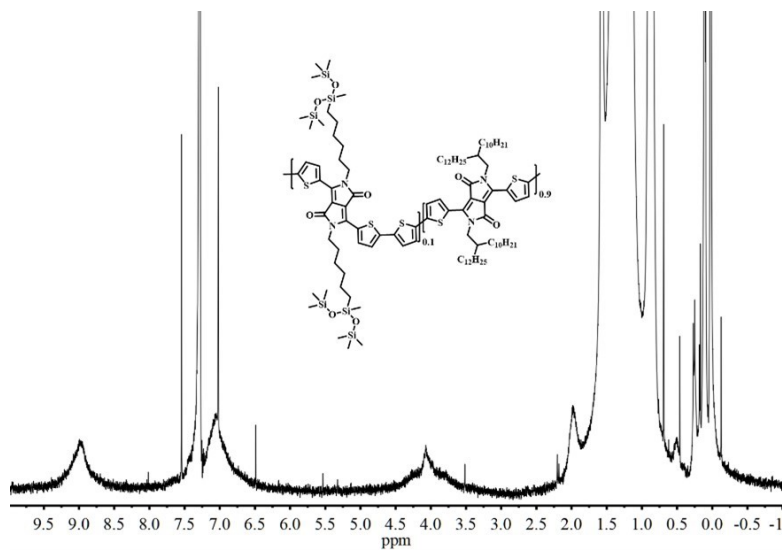


**Fig. S5.** <sup>1</sup>H NMR spectrum of polymer PDPPSi<sub>10</sub>.



The NMR spectra of PDPPSi<sub>10</sub> (black bulk solid, 51% yield) is shown in **Fig. S5**, <sup>1</sup>H NMR (400 MHz, CDCl<sub>3</sub>) δ 8.99 (s, 2H), 7.02 (s, 4H), 4.07 (s, 4H), 1.88-0.34 (m, alkyl).

**PDPPSi<sub>30</sub>**

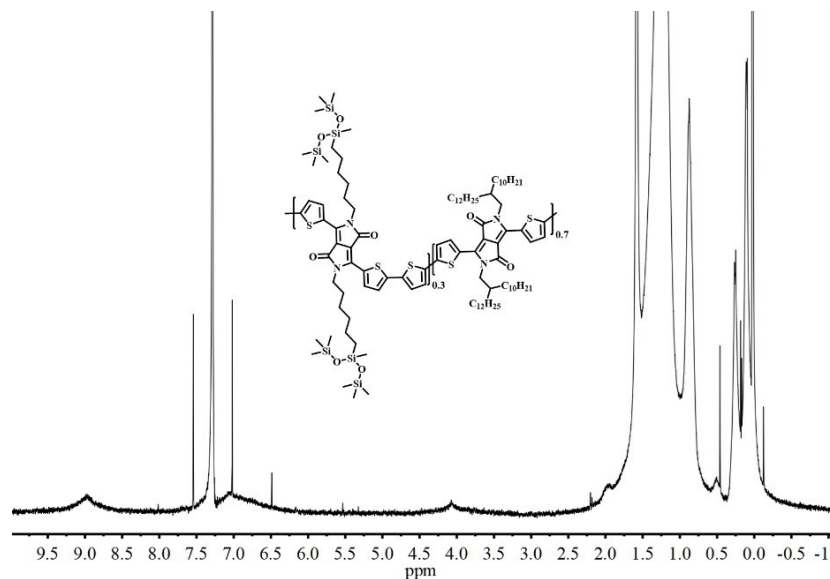


**Fig. S6.** <sup>1</sup>H NMR spectrum of polymer PDPPSi<sub>30</sub>.

The NMR spectra of PDPPSi<sub>30</sub> (black bulk solid, 49% yield) is shown in **Fig. S6**, <sup>1</sup>H NMR (400 MHz, CDCl<sub>3</sub>) δ 8.98 (s, 2H), 7.02 (s, 4H), 4.07 (s, 4H), 2.01-0.45 (m, alkyl).

***PDPPSi<sub>50</sub>***

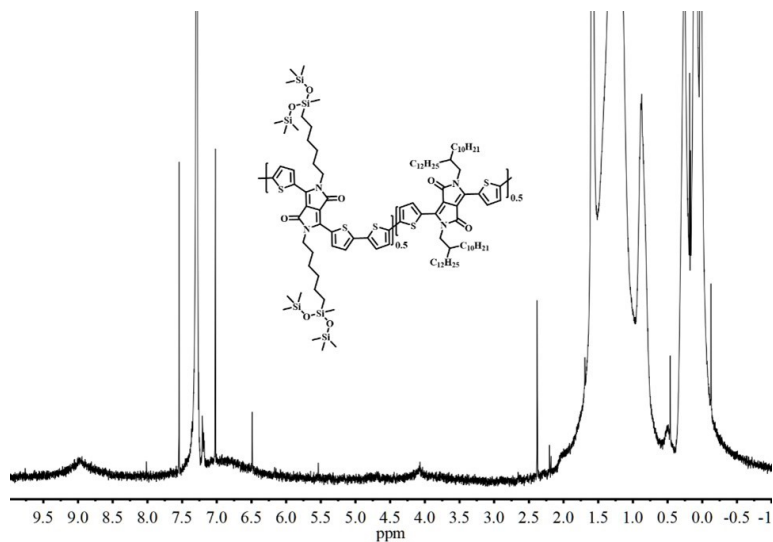


**Fig. S7.** <sup>1</sup>H NMR spectrum of polymer PDPPSi<sub>50</sub>.

The NMR spectra of PDPPSi<sub>50</sub> (black bulk solid, 53% yield) are shown in **Fig. S7**, <sup>1</sup>H NMR (400 MHz, CDCl<sub>3</sub>) δ 8.95 (s, 2H), 7.02 (s, 4H), 4.08 (s, 4H), 2.27-0.91 (m, alkyl).

***PDPPSi<sub>70</sub>***

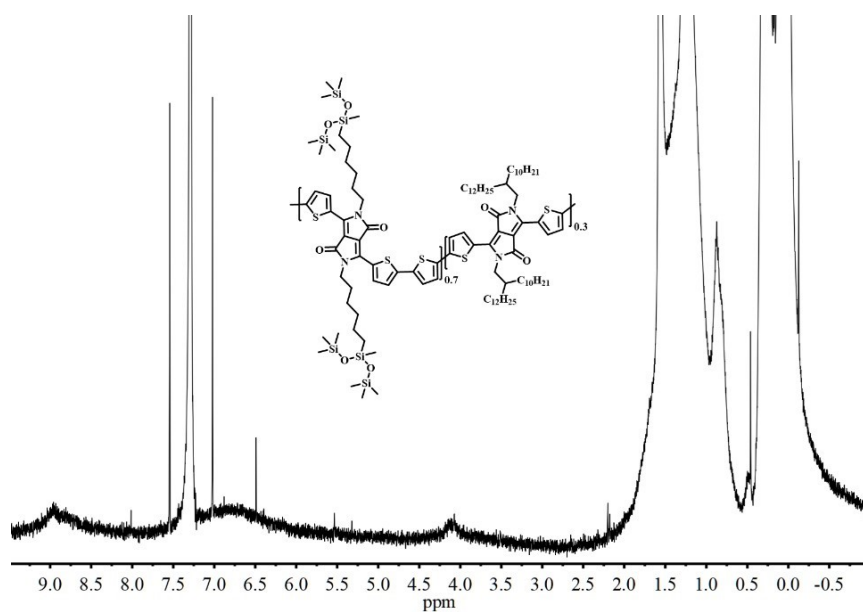


**Fig. S8.** <sup>1</sup>H NMR spectrum of polymer PDPPSi<sub>70</sub>.

The NMR spectra of PDPPSi<sub>70</sub> (black bulk solid, 50% yield) are shown in **Fig. S8**, <sup>1</sup>H NMR (400 MHz, CDCl<sub>3</sub>) δ 8.96 (s, 2H), 7.02 (s, 4H), 4.07 (s, 4H), 2.14-0.79 (m, alkyl).

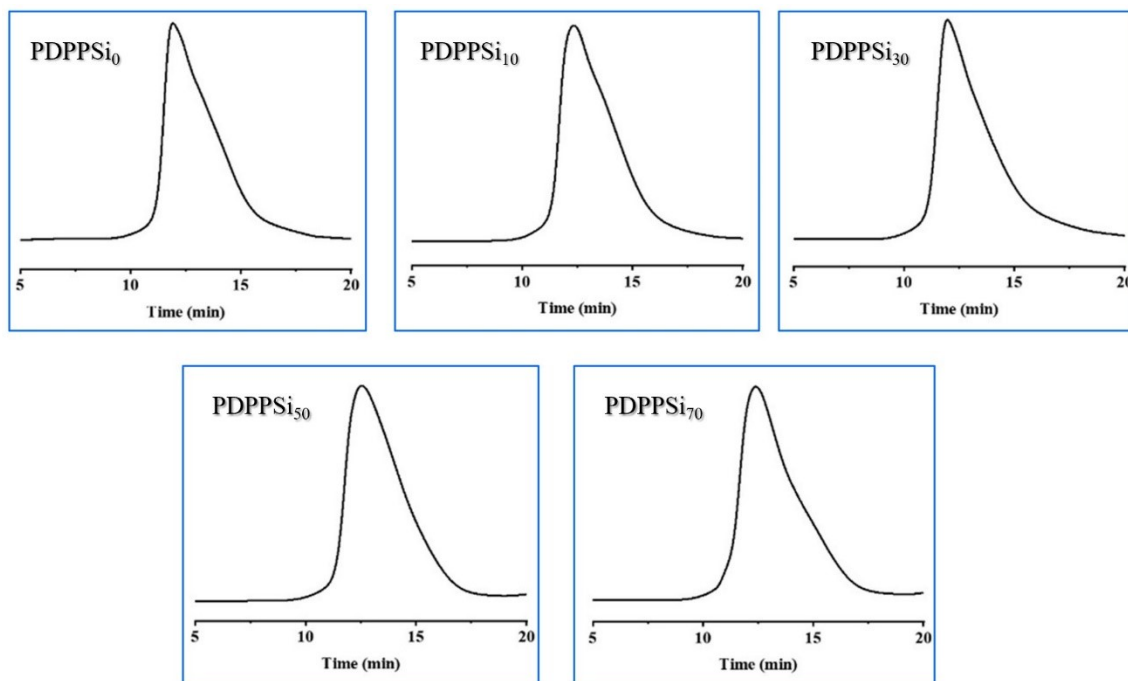


**Fig. S9.** GPC curves of the PDPPSi<sub>x</sub> polymers.

#### **S1.4. Electrochemical properties of the DPP polymers**

The electrochemical properties of five polymers were characterized by cyclic voltammetry (CV). The three-electrode method was used to determine the energy levels of the polymer, in which platinum was the working electrode, Ag/Ag<sup>+</sup> was the reference electrode, platinum wire was the reverse electrode, and 0.1 M · L<sup>-1</sup> tetrabutylammonium hexafluorophosphate (Bu<sub>4</sub>NPF<sub>6</sub>) anhydrous acetonitrile solution was the electrolyte. Before the test, the electrolyte was bubbled with nitrogen

for 30 min to remove oxygen in the electrolyte, and the test was carried out in a nitrogen atmosphere.

The voltammetry curves (CVs) of five polymers and ferrocene are shown in **Fig. S10a**. The initial oxidation potential ( $E_{\text{ox}}^{\text{onset}}$ ) of five kinds of polymers was obtained by testing, and the oxidation potential of five kinds of polymers was calibrated using the standard potential ferrocene ( $E_{\text{ferrocene}}^{\text{onset}}$ ). The formula for calculating the HOMO energy level of polymers is generally as follows:  $E_{\text{HOMO}} = - \left[ 4.8 + \left( E_{\text{ox}}^{\text{onset}} - E_{1/2(\text{Fc}/\text{Fc}^+)} \right) \right] \text{ eV}$ . The HOMO energy levels of the five polymers are -5.35, -5.25, -5.25, -5.21, and -5.11 eV, respectively, as shown in **Fig. S10b**. According to the Tauc plot method, the optical band gaps of five polymers were calculated by ultraviolet spectroscopy, as shown in **Fig. 6a** (See the manuscript). The polymers in the chlorobenzene/o-dichlorobenzene (1:1 volume ratio) mixture were shown in equation 1:

$$(\alpha h\nu)^m = B(h\nu - E_g) \quad (1)$$

where  $\alpha$  is the absorption coefficient,  $h$  is Planck's constant,  $\nu$  is the frequency of the incident photon,  $B$  is the constant,  $E_g$  is the bandgap (band gap) of the semiconductor, and the value of  $m$  is related to the semiconductor material and the transition type,  $m = 2$  corresponds to the allowable dipole transition of the direct bandgap semiconductor, and  $m = 1/2$  corresponds to the allowable transition of the indirect bandgap semiconductor. The optical bandgaps corresponding to the five polymers were  $E_g$ , PDPPSi<sub>0</sub> = 1.41 eV,  $E_g$ , PDPPSi<sub>10</sub> = 1.42 eV,  $E_g$ , PDPPSi<sub>30</sub> = 1.40 eV,  $E_g$ , PDPPSi<sub>50</sub> = 1.38 eV,  $E_g$ , PDPPSi<sub>70</sub> = 1.34 eV (as shown in **Fig. S10c**).

The formula  $E_{\text{LUMO}} = E_g + E_{\text{HOMO}}$  was determined the LUMO energy levels of the five polymers were -3.94 eV, -3.83 eV, -3.85 eV, -3.83 eV, and -3.77 eV, respectively **Fig. S10b**.

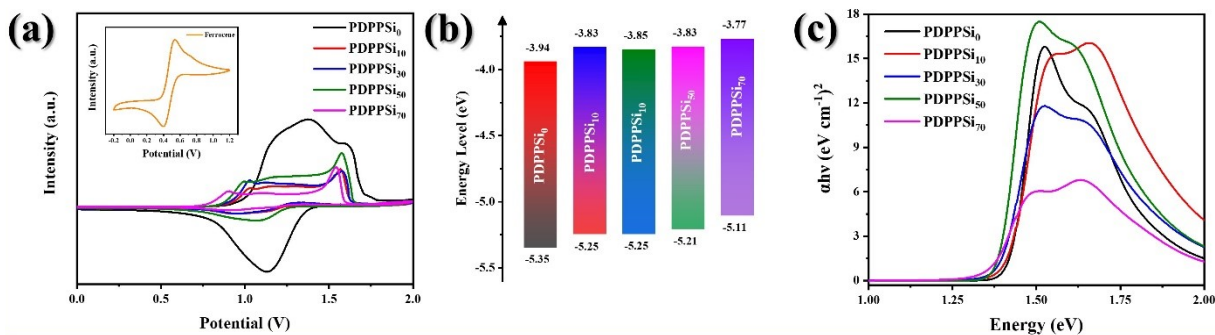


**Fig. S10.** (a) Cyclic voltammetry curve of polymers PDPPSi<sub>0</sub>, PDPPSi<sub>10</sub>, PDPPSi<sub>30</sub>, PDPPSi<sub>50</sub>, PDPPSi<sub>70</sub> and ferrocene (inserted), (b) HOMO and LUMO energy levels, and (c) Linear relation curve of  $(\alpha h\nu)^2 - h\nu$  of polymers.

**Table S1.** The main absorption peaks of polymers in solution and film states.

Polymer	$\lambda_{\text{solution}}$ (nm)	$\lambda_{\text{film}}$ (nm)
PDPPSi <sub>0</sub>	400/817	418/829
PDPPSi <sub>10</sub>	394/802	420/830
PDPPSi <sub>30</sub>	396/818	418/838
PDPPSi <sub>50</sub>	408/828	418/842
PDPPSi <sub>70</sub>	412/838	418/832

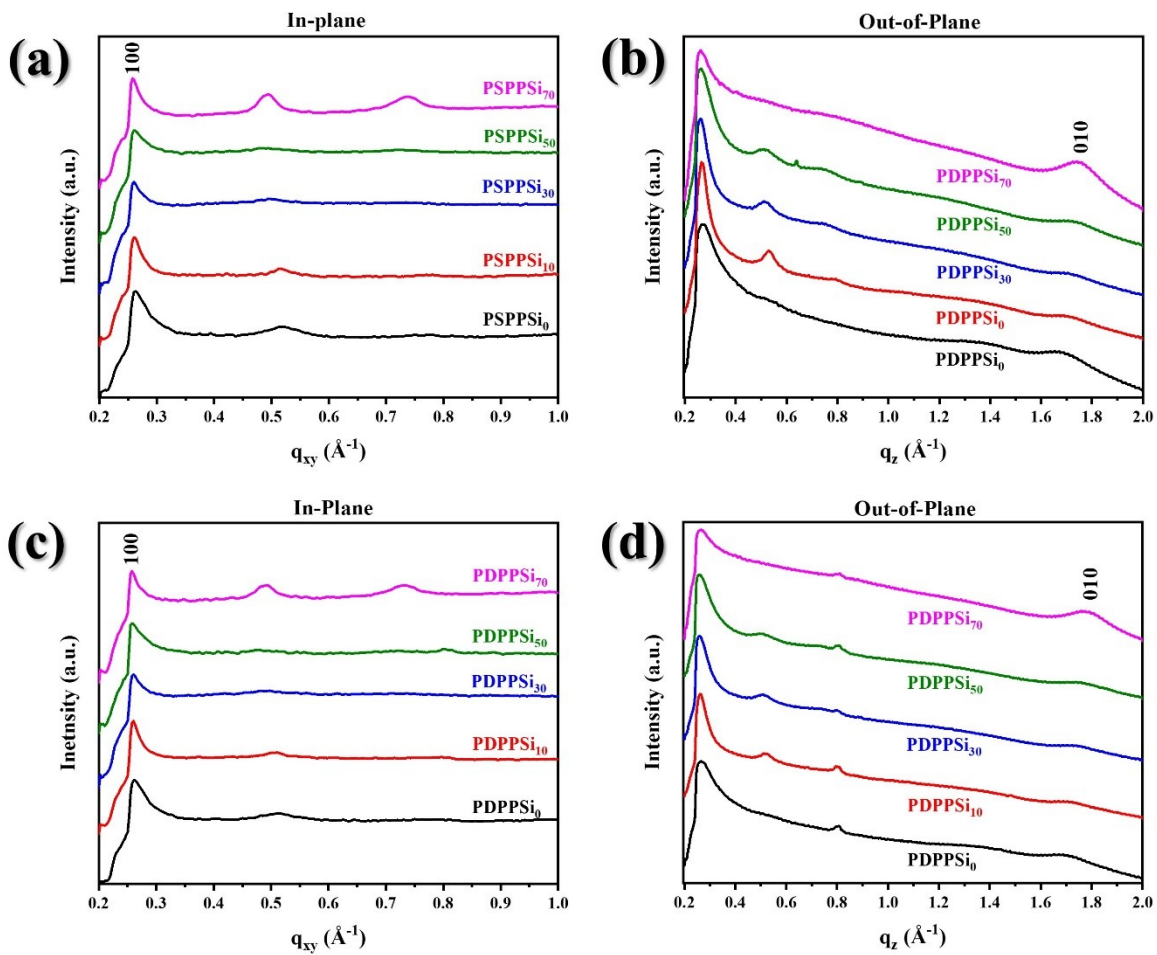


**Fig. S11.** In-plane and Out-of-Plane 1D XRD patterns of (a, b) Undoped and (c, d) FeCl<sub>3</sub>-doped PDPPSi<sub>x</sub> polymers obtained from 2D GIWAX patterns.

**Table S2.** The data of peaks position,  $d$ -spacing and  $\pi$ - $\pi$  stacking distance of undoped and FeCl<sub>3</sub>-doped PDPPSi<sub>*x*</sub> polymers.

Polymer	In-Plane				Out-of-Plane			
	Lamella Packing (100)				$\pi$ - $\pi$ stacking (010)			
	Undoped		Fe-Cl <sub>3</sub> -Doped		Undoped		Fe-Cl <sub>3</sub> -Doped	
	$q_{xy}(\text{\AA}^{-1})$	$d$ -spacing (Å)	$q_{xy}(\text{\AA}^{-1})$	$d$ -spacing (Å)	$q_z(\text{\AA}^{-1})$	$\pi$ - $\pi$ stacking (Å)	$q_z(\text{\AA}^{-1})$	$\pi$ - $\pi$ stacking (Å)
PDPPSi <sub>0</sub>	0.265	23.71	0.265	23.71	1.655	3.7965	1.6725	3.7568
PDPPSi <sub>10</sub>	0.265	23.71	0.265	23.94	1.6875	3.7234	1.7	3.6960
PDPPSi <sub>30</sub>	0.265	23.94	0.265	24.17	1.705	3.6852	1.72	3.6530
PDPPSi <sub>50</sub>	0.265	23.94	0.265	24.17	1.715	3.6637	1.7425	3.6058
PDPPSi <sub>70</sub>	0.265	23.94	0.265	23.71	1.6925	3.7124	1.76	3.5700

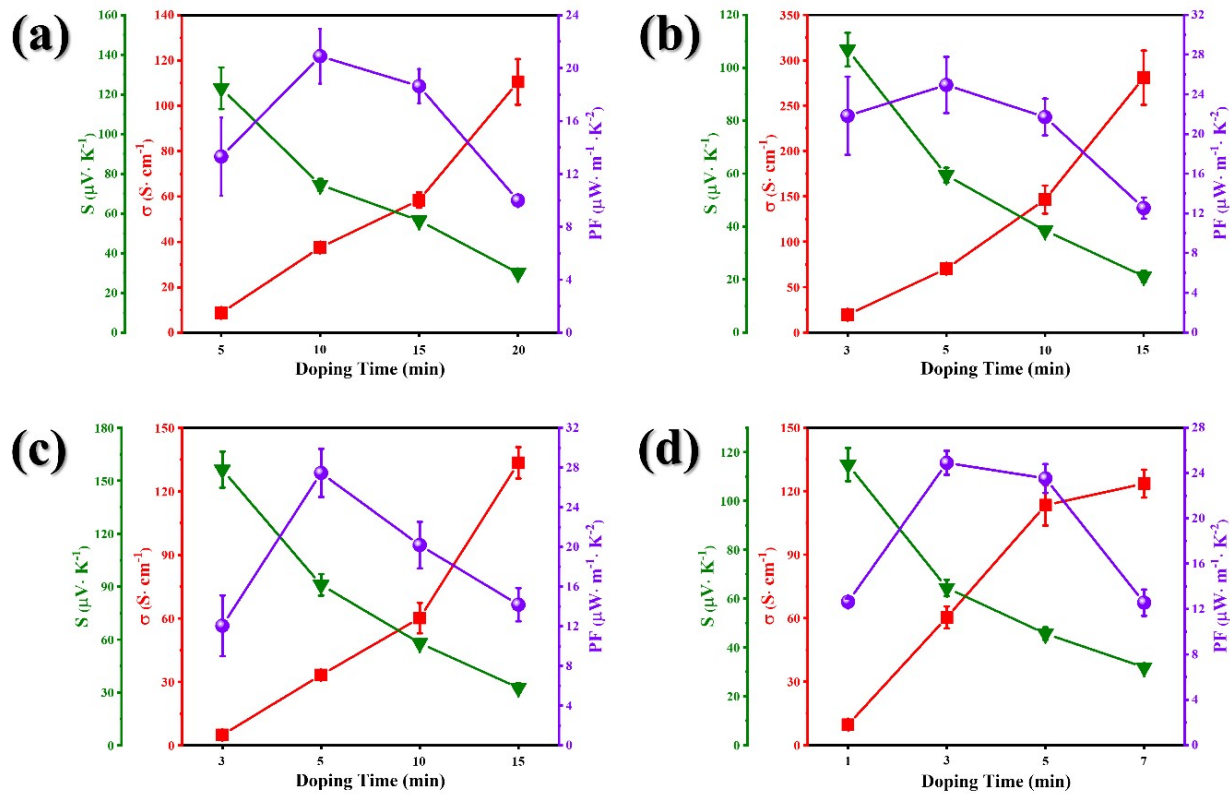


**Fig. S12.** The thermoelectric performance of the FeCl<sub>3</sub>-doped (a) PDPPSi<sub>0</sub>, (b) PDPPSi<sub>10</sub>, (c) PDPPSi<sub>30</sub>, and (d) PDPPSi<sub>70</sub> polymer films.